JCI The Journal of Clinical Investigation

Extracellular K^+ concentration controls cell surface density of I_{Kr} in rabbit hearts and of the HERG channel in human cell lines

Jun Guo, … , Nasrin Mesaeli, Shetuan Zhang

J Clin Invest. 2009;119(9):2745-2757. https://doi.org/10.1172/JCI39027.

Research Article

Although the modulation of ion channel gating by hormones and drugs has been extensively studied, much less is known about how cell surface ion channel expression levels are regulated. Here, we demonstrate that the cell surface density of both the heterologously expressed K^+ channel encoded by the human ether-a-go-go–related gene (*HERG*) and its native counterpart, the rapidly activating delayed rectifier K^+ channel (I_{Kr}), in rabbit hearts in vivo is precisely controlled by extracellular K^+ concentration ($[K^+]_o$) within a physiologically relevant range. Reduction of $[K^+]_o$ led to accelerated internalization and degradation of HERG channels within hours. Confocal analysis revealed colocalization between HERG and ubiquitin during the process of HERG internalization, and overexpression of ubiquitin facilitated HERG degradation under low $[K^+]_o$. The HERG channels colocalized with a marker of multivesicular bodies during internalization, and the internalized HERG channels were targeted to lysosomes. Our results provide the first evidence to our knowledge that the cell surface density of a voltage-gated K^+ channel, HERG, is regulated by a biological factor, extracellular K^+. Because hypokalemia is known to exacerbate long QT syndrome (LQTS) and Torsades de pointes tachyarrhythmias, our findings provide a potential mechanistic link between hypokalemia and LQTS.

Extracellular K^+ concentration controls cell surface density of I_{Kr} in rabbit hearts and of the HERG channel in human cell lines

Jun Guo,[1] Hamid Massaeli,[1] Jianmin Xu,[1] Zongchao Jia,[2] Jeffrey T. Wigle,[3,4] Nasrin Mesaeli,[3,4] and Shetuan Zhang[1]

[1]Department of Physiology and [2]Department of Biochemistry, Queen's University, Kingston, Ontario, Canada. [3]Institute of Cardiovascular Sciences, St. Boniface General Hospital Research Centre, Winnipeg, Manitoba, Canada. [4]Department of Biochemistry and Medical Genetics, University of Manitoba, Winnipeg, Manitoba, Canada.

Although the modulation of ion channel gating by hormones and drugs has been extensively studied, much less is known about how cell surface ion channel expression levels are regulated. Here, we demonstrate that the cell surface density of both the heterologously expressed K^+ channel encoded by the human ether-a-go-go–related gene (*HERG*) and its native counterpart, the rapidly activating delayed rectifier K^+ channel (I_{Kr}), in rabbit hearts in vivo is precisely controlled by extracellular K^+ concentration ($[K^+]_o$) within a physiologically relevant range. Reduction of $[K^+]_o$ led to accelerated internalization and degradation of HERG channels within hours. Confocal analysis revealed colocalization between HERG and ubiquitin during the process of HERG internalization, and overexpression of ubiquitin facilitated HERG degradation under low $[K^+]_o$. The HERG channels colocalized with a marker of multivesicular bodies during internalization, and the internalized HERG channels were targeted to lysosomes. Our results provide the first evidence to our knowledge that the cell surface density of a voltage-gated K^+ channel, HERG, is regulated by a biological factor, extracellular K^+. Because hypokalemia is known to exacerbate long QT syndrome (LQTS) and Torsades de pointes tachyarrhythmias, our findings provide a potential mechanistic link between hypokalemia and LQTS.

Introduction

The amplitude of ion channel currents is determined by a combination of channel gating (open versus closed times) and channel density in the plasma membrane. Whereas ion channel gating is known to be modulated by various means, such as hormones and drugs, much less is known about how the density of WT ion channels in the plasma membrane is regulated.

The human ether-a-go-go–related gene (*HERG*) encodes the pore-forming subunits of the rapidly activating delayed rectifier K^+ channel (I_{Kr}) in the heart (1, 2). Mutations in *HERG* reduce I_{Kr} and cause type 2 long QT syndrome (LQT2), a disorder that predisposes individuals to life-threatening arrhythmias (3). In addition, the HERG channel is a common target for diverse classes of drugs that induce acquired long QT syndrome (LQTS; ref. 4). Whereas drugs usually reduce HERG channel current (I_{HERG}) by blocking the channel, LQTS-causing HERG mutations often decrease I_{HERG} by disrupting forward trafficking of the channel, thereby reducing expression levels of HERG at the plasma membrane (5). However, little is presently known about how the plasma membrane density of WT HERG channels is regulated under either physiological or pathophysiological conditions.

Disorders of extracellular K^+ concentration ($[K^+]_o$) are the most common electrolyte abnormality found in clinical practice and can be life threatening. For example, abrupt, insulin-induced shifts of K^+ from the extracellular compartment into cells, abnormal K^+ losses caused by digestive or kidney disorders, and the use of certain diuretics are common causes of low $[K^+]_o$ (hypokalemia). It is also known that hypokalemia exacerbates LQTS and Torsades de pointes tachyarrhythmias (6) and that moderate increases in serum $[K^+]$ can correct LQTS in certain patients (7, 8). Therefore, hypokalemia is an important risk factor for LQTS and sudden cardiac death.

In the present study, we investigated the chronic effects of $[K^+]_o$ on HERG channel function and expression in a stable HERG-expressing HEK 293 cell line (HERG-HEK) and on native I_{Kr} in a hypokalemia rabbit model in vivo. Our data demonstrated that lowering $[K^+]_o$ drastically accelerated HERG internalization and degradation such that the density of HERG channels in the plasma membrane was precisely controlled by $[K^+]_o$. This finding of HERG channel density regulation in the cell membrane by $[K^+]_o$ extends our understanding of ion channel biology and provides a potential mechanism for hypokalemia-induced exacerbation of LQTS.

Results

Chronic alterations of $[K^+]_o$ regulate HERG current. Hypokalemia prolongs cardiac action potential duration (9). We investigated the effects of lowering $[K^+]_o$ in the culture medium on the function of HERG, human ether-a-go-go (EAG), KvLQT1 plus KCNE1 (which encode slowly activating delayed rectifier K^+ channel current; KCNE1 is also known as MinK), or Kv1.5 (which encodes ultra-rapidly activating delayed rectifier K^+ channel current) K^+ channels stably expressed in HEK 293 cells (Figure 1A). In order to precisely manipulate $[K^+]_o$, we used a custom 0 mM K^+ MEM that lacked K^+ in any form but contained all other components of standard MEM. Because FBS contains K^+, FBS was not included in the culture medium in the experiments unless otherwise indicated. After overnight (12 hours) exposure of cells to 0 or 5 mM K^+ MEM, each distinct K^+ current was recorded using the whole-cell clamp method with a standard 5 mM K^+–containing bath solu-

Authorship note: Jun Guo and Hamid Massaeli contributed equally to this work.
Conflict of interest: The authors have declared that no conflict of interest exists.
Citation for this article: *J. Clin. Invest.* **119**:2745–2757 (2009). doi:10.1172/JCI39027.

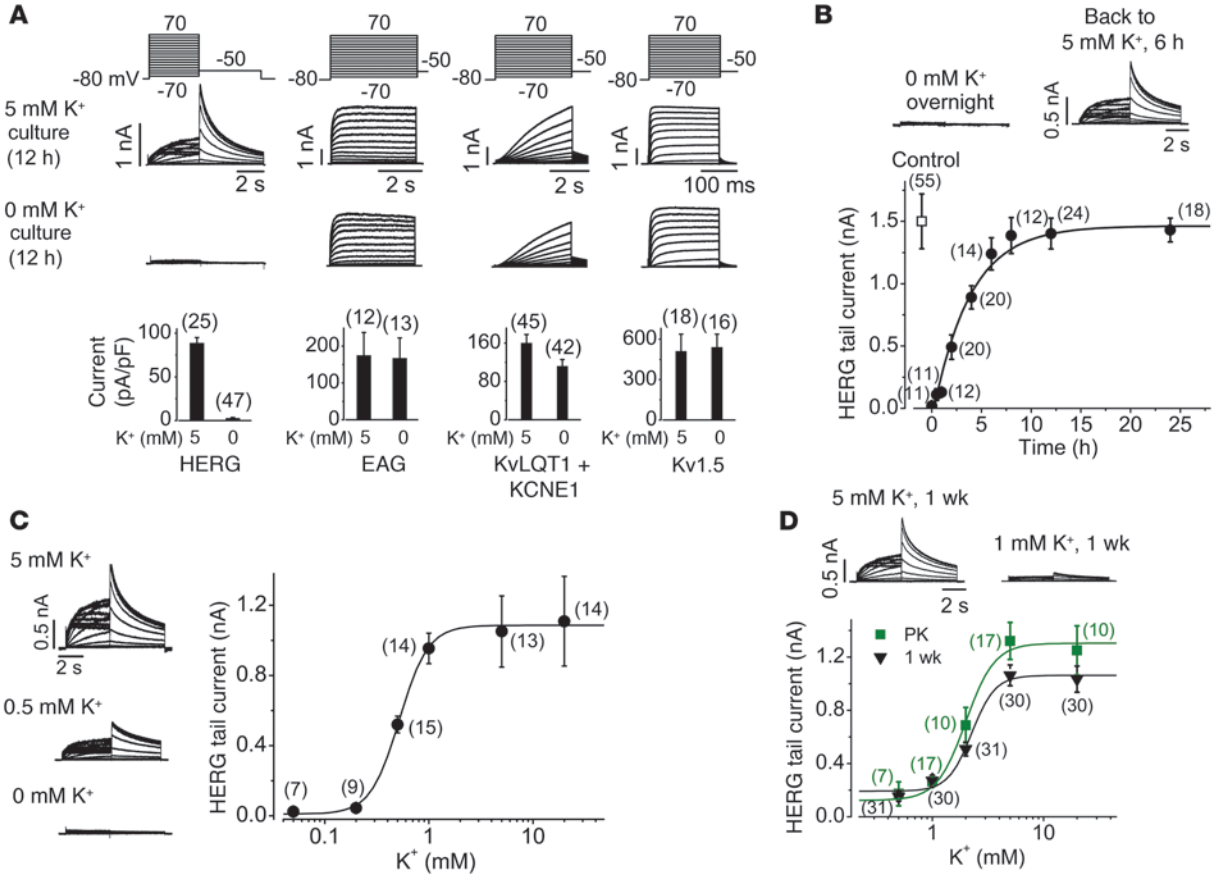

Figure 1

The $[K^+]_o$ of the incubation medium dictates amplitude of the HERG current. (**A**) Effects of overnight exposure to 0 mM K^+ MEM on the HERG, EAG, KvLQT1 plus KCNE1, and Kv1.5 channel currents. Voltage protocols are shown above the current traces, and the relative reductions of various channel currents are shown below. Current amplitude was measured by tail current at –50 mV after 50-mV depolarizing steps for the HERG channel, or by pulse current at the end of a depolarizing step to 70 mV for the EAG, KvQLT1 plus KCNE1, and Kv1.5 channels. (**B**) Time-dependent recovery of I_{HERG} in 5 mM K^+ MEM from overnight exposure to 0 mM K^+ MEM. (**C**) Concentration-dependent effects of K^+_o on I_{HERG} after overnight culture. (**D**) Concentration-dependent effects of K^+_o on I_{HERG} after 1 week culture of HERG-HEK cells (black) or after 32–36 hours of culture of proteinase K–treated HERG-HEK cells (PK; green). All HERG currents shown in **B**–**D** were recorded using the same voltage protocol as in **A**. Numbers in parentheses denote *n* from at least 3 independent experiments.

tion and a 135 mM K^+–containing pipette solution (see Methods). Currents were elicited by depolarizing steps between –70 mV and +70 mV in 10-mV increments, followed by a repolarizing step to –50 mV to record tail currents. Overnight exposure to 0 mM K^+ MEM completely eliminated I_{HERG} (Figure 1A). However, there was no change in the EAG or Kv1.5 currents, and a modest reduction (by 30.3% ± 8%) in the KvLQT1 plus KCNE1 current, in response to the same treatment (Figure 1A). The 0 mM K^+–induced I_{HERG} reduction was fully reversible: after complete loss of I_{HERG} caused by overnight exposure to 0 mM K^+ MEM, addition of 5 mM K^+ to the MEM restored I_{HERG} with a single exponential time constant of 3.7 hours (Figure 1B). Thus, the presence of extracellular K^+ (K^+_o) is a prerequisite for normal HERG channel function.

To quantify $[K^+]_o$ effects on I_{HERG}, we cultured HERG-HEK cells overnight in MEM with various $[K^+]_o$. Altering $[K^+]_o$ modified I_{HERG} in a concentration-dependent manner with an EC_{50} of 0.56 ± 0.06 mM and a Hill coefficient (H) of 3.4 (Figure 1C). In contrast to the effects on amplitude, varying $[K^+]_o$ in MEM did not alter the gating kinetics of I_{HERG}. For example, the voltage for half-maximal activation and the slope factor of HERG channels was –10.7 ± 1.1 mV and 8.4 ± 1.0 mV, respectively, in cells under 5 mM K^+ culture (n = 6), and –9.9 ± 1.7 mV (P > 0.05) and 8.9 ± 0.9 mV (P > 0.05), respectively, in cells under 0.5 mM K^+ culture for 12 hours (n = 6). Thus, alterations in $[K^+]_o$ in cell culture medium is likely to affect the number of functional channels.

It was previously reported that HERG associates with KCNE1 or KCNE2 (also known as MIRP1) polypeptides (10, 11). To determine whether KCNE1 or KCNE2 plays a role in the $[K^+]_o$ dependence of I_{HERG}, we expressed either KCNE1 or KCNE2 in HERG-HEK cells. A plasmid encoding GFP was cotransfected to select for transfected cells in patch-clamp experiments. Expression of KCNE1 and KCNE2 was confirmed using Western blot analysis. As summarized in Supplemental Figure 1 (supplemental material available online with this article; doi:10.1172/JCI39027DS1), we did not detect any major effects of either KCNE1 or KCNE2 coexpression on HERG gating kinetics. Importantly, coexpression of KCNE1 or KCNE2 with HERG did not alter the $[K^+]_o$ dependence of I_{HERG} (Supplemental Figure 1). Specifically, overnight exposure

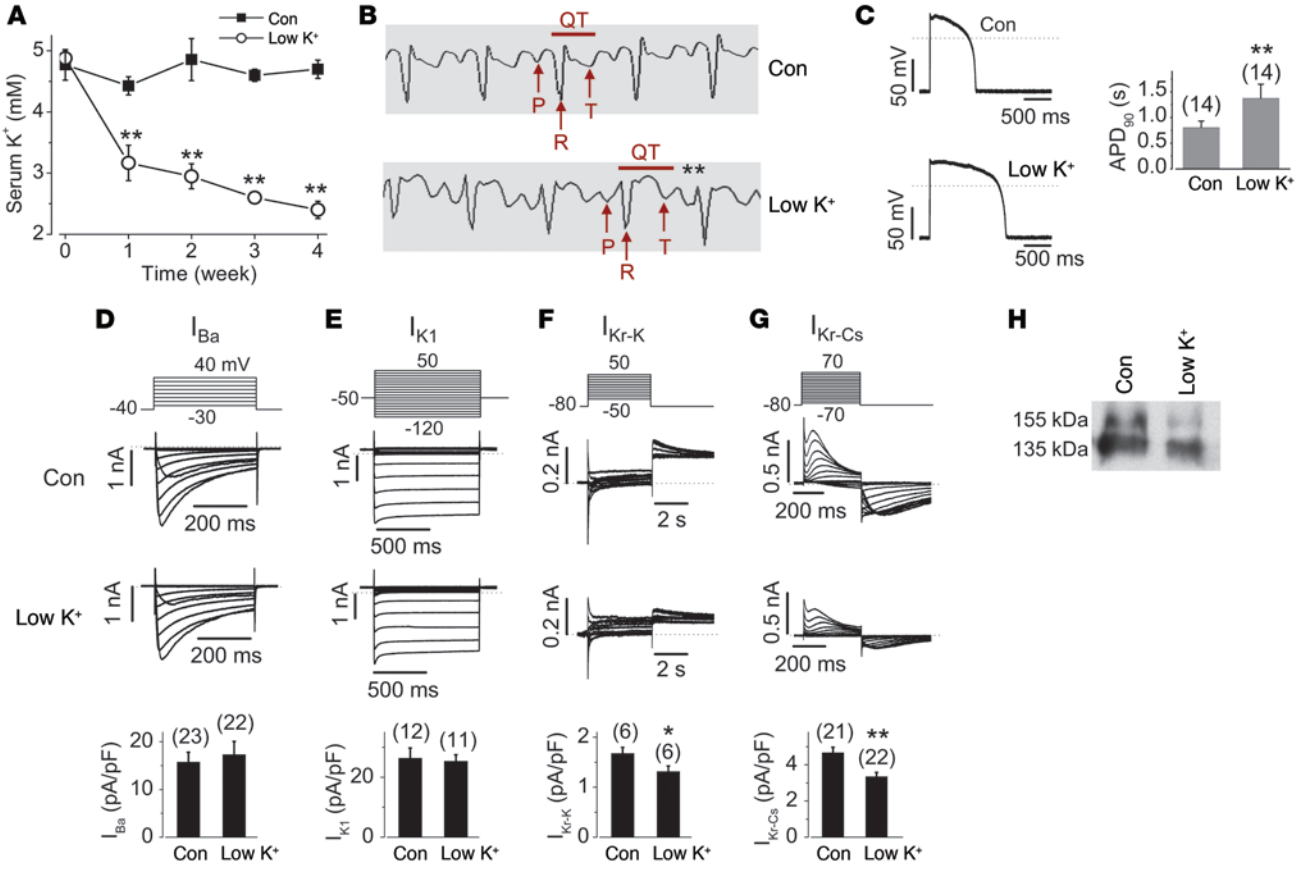

Figure 2

Decrease in serum [K+] reduces I_{Kr} and its mature 155-kDa form in rabbit hearts. (**A**) Serum [K+] in rabbits fed a control (n = 7) or a low-K+ diet (n = 9). (**B**) Representative ECG traces from control diet– or low-K+ diet–fed rabbits. The QT interval denotes the period from the start of the QRS complex to the end of the T wave (peaks of P, R, and T waves are indicated by arrows). (**C**) Action potentials recorded in ventricular myocytes from control diet– or low-K+ diet–fed rabbits. The stimulation interval was 5 seconds. (**D**–**G**) Ba^{2+}-mediated L-type Ca^{2+} channel current (I_{Ba}; **D**), I_{K1} (**E**), K+-mediated I_{Kr} ($I_{Kr\text{-}K}$; **F**), and Cs^+-mediated I_{Kr} ($I_{Kr\text{-}Cs}$; **G**) recorded in ventricular myocytes from control diet– and low-K+ diet–fed rabbits. Voltage protocols are shown above the corresponding current traces. The amplitude of I_{Ba} at 0 mV, I_{K1} at the end of the test voltage –120 mV, outward tail current of $I_{Kr\text{-}K}$ at –50 mV, and inward tail of $I_{Kr\text{-}Cs}$ at –80 mV were used for statistical analyses between groups. (**H**) I_{Kr} expression levels of the membrane proteins from ventricles of control diet– or low-K+ diet–fed rabbits. Similar results were obtained in 5 rabbits per group. $^*P < 0.05$, $^{**}P < 0.01$ versus control. Numbers in parentheses denote n from at least 3 independent experiments.

to 0 mM K^+ reduced I_{HERG} by 97.4% ± 1.9% (n = 25 versus 47 cells; Figure 1A), reduced $I_{HERG+KCNE1}$ by 91.4% ± 9% (n = 11 versus 12 cells; $P > 0.05$), and reduced $I_{HERG+KCNE2}$ by 92.4% ± 5.2% (n = 7 versus 9 cells; $P > 0.05$; Supplemental Figure 1).

The above results raised the possibility that HERG channels require K^+_o to maintain their membrane stability, and that lowering $[K^+]_o$ decreases cell membrane HERG density. Presumably, this could occur by destabilizing HERG membrane localization and thereby promoting its degradation (see below). In order to determine the physiological relevance of K^+_o regulation of HERG channels, we investigated the steady-state effects of $[K^+]_o$ on HERG function. Because our stable HERG-HEK cell line was maintained in a normal culture MEM with a [K+] of 5 mM, which sustained the maximum channel density (Figure 1C), the EC_{50} of $[K^+]_o$ required for maintaining I_{HERG} would be underestimated if steady-state I_{HERG} was not reached after 12 hours of culture at a $[K^+]_o$ level less than 5 mM. To examine this notion, we determined the reduction of I_{HERG} after switching $[K^+]_o$ in MEM from 5 to 0.5 mM for 6, 12, and 24 hours. I_{HERG} decreased to 66.3% at 6 hours (n = 12), 46.3% at 12 hours (n = 13), and 31.2% at 24 hours (n = 14; $P < 0.01$ versus 12 hours), indicating that the I_{HERG} is reduced in a time-dependent manner, does not reach steady state in 12 hours, and requires a higher $[K^+]_o$ to maintain 50% functional HERG channels after 24 hours' exposure.

In order to obtain a steady-state effect of $[K^+]_o$ on I_{HERG}, we cultured HERG-HEK cells in variable $[K^+]_o$ for 1–3 weeks. For long-term cell cultures, FBS is required for cell survival. Because FBS contains 11 mM K^+, a baseline medium with 0.5 mM K^+ was made by adding 4.5% FBS to 0 mM K^+ MEM. FBS did not alter $[K^+]_o$ dependence of I_{HERG}, as no significant difference was observed for I_{HERG} reduction upon overnight exposure to FBS-containing 0.5 mM K^+ MEM (38.8% ± 7.8%; n = 10) or FBS-free 0.5 mM K^+ MEM (42.5% ± 6.7%; n = 11; $P > 0.05$). After 1 week of culture, I_{HERG} displayed $[K^+]_o$ dependence, with an EC_{50} of 2.1 ± 0.3 mM (H, 3.1; Figure 1D). We further cultured HERG-HEK cells for 2 and 3 weeks in different $[K^+]_o$; the EC_{50} of $[K^+]_o$ for regulating I_{HERG} was 2.8 ± 0.6 (H, 4; 10–11 cells

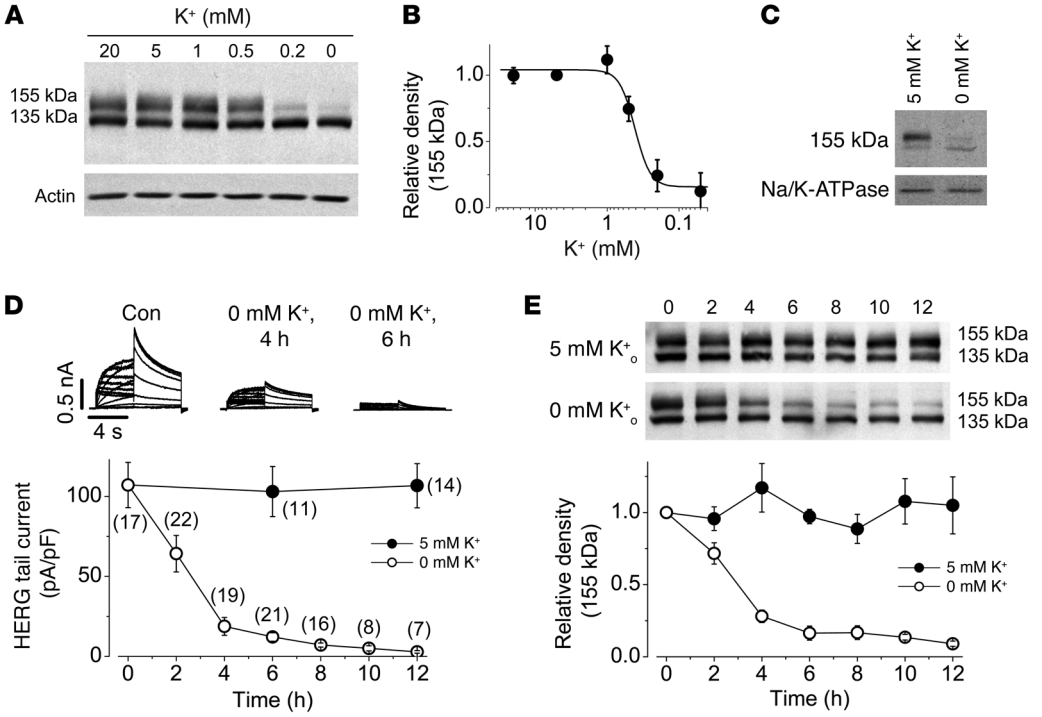

Figure 3

The $[K^+]_o$ controls HERG membrane expression. (**A** and **B**) Concentration-dependent effects of K^+_o, after overnight exposure, on (**A**) HERG channel expression levels and (**B**) relative intensity of the 155-kDa band. (**B**) The intensity of the 155-kDa band at each $[K^+]_o$ was normalized to the value at 5 mM K^+ and plotted against $[K^+]_o$. (**C**) Effects of $[K^+]_o$ on cell surface HERG expression. Surface proteins from HERG-HEK cells cultured in 0 or 5 mM K^+ for 12 hours were isolated and analyzed by Western blot using an anti-HERG antibody. For statistical analysis (see Results), the intensity of the 155-kDa band in 0 mM K^+ was normalized to its pair in 5 mM K^+ for each set of 3 experiments. Na/K-ATPase (100 kDa), detected using an anti–Na/K-ATPase antibody, was used as a loading control for isolated cell surface proteins. (**D** and **E**) Time-dependent effects of exposure to 0 or 5 mM K^+ MEM on I_{HERG} (**D**) or on HERG protein expression levels (**E**). The HERG currents were recorded using the protocol shown in Figure 1A. (**E**) Intensities of the 155-kDa bands in 0 or 5 mM K^+ at each time point were normalized to their initial values and plotted as a function of time. Numbers in parentheses denote *n* from at least 3 independent experiments.

at each $[K^+]_o$) and 1.8 ± 0.1 mM (H, 3.2; 10–11 cells at each $[K^+]_o$), respectively. Thus, the effects of $[K^+]_o$ on I_{HERG} attained steady state within 1 week, and preexisting HERG maximum membrane expression was responsible for the difference of EC_{50} between overnight and 1-week treatment of cells. To study the $[K^+]_o$ dependence of HERG membrane expression in the absence of preexisting HERG channels in the stable HERG cell line, we eliminated cell surface HERG channels by treating live cells with externally applied proteinase K. Several investigators, including us, have previously demonstrated that treating live HERG-HEK cells with external proteinase K completely removes the cell surface HERG channels (12, 13). After proteinase K treatment, the newly synthesized HERG channels accumulate on the plasma membrane with a time constant of 13.2 hours and approach a maximum within 32 hours (12). In this situation, the membrane density of newly synthesized HERG channels from cells cultured in variable $[K^+]_o$ would directly reflect the $[K^+]_o$ dependence of HERG channel membrane stability. We treated HERG-HEK cells with proteinase K, confirmed complete removal of cell surface HERG using patch-clamp recordings, and cultured the treated cells for 32–36 hours in various $[K^+]$ MEM. The EC_{50} of $[K^+]_o$ for regulating I_{HERG} was 2.0 ± 0.2 mM (H, 3.4; Figure 1D), comparable to the EC_{50} from cells after 1 week of culture. Thus, K^+_o is required for HERG function, and $[K^+]_o$ fluctuations under pathophysiological conditions may regulate I_{Kr} in vivo.

Hypokalemia prolongs QT interval and decreases I_{Kr} in rabbits. To study the effects of lowering $[K^+]_o$ on I_{Kr} in vivo, we fed rabbits either a control or a low-K^+ diet. The compositions of both diets were identical except for K^+ content (control, 0.62%; low K^+, 0.1%). Serum $[K^+]$ in rabbits fed the low-K^+ diet dropped significantly after 1 week and continued to decrease during 4 weeks on the same diet (Figure 2A). After 4 weeks, serum $[K^+]$ remained stable in rabbits fed the control diet (4.69 ± 0.15 mM, versus 4.77 ± 0.25 mM before feeding; $n = 7$), but decreased significantly in rabbits fed the low-K^+ diet (2.40 ± 0.14 mM, versus 4.88 ± 0.13 mM before feeding; $n = 9$; $P < 0.01$). The corrected QT intervals ($QT/[RR]^{1/2}$) were significantly prolonged, from 0.27 ± 0.02 seconds in control rabbits ($n = 7$) to 0.36 ± 0.01 seconds in rabbits fed the low-K^+ diet ($n = 9$; $P < 0.01$; Figure 2B). Heart rate was not different between control and low-K^+ diet groups (control, 268 ± 18 bpm, $n = 7$; low K^+, 246 ± 5 bpm, $n = 9$; $P > 0.05$). To determine the ionic mechanisms for the prolonged QT intervals, we recorded action potentials and various ionic currents in single ventricular myocytes isolated from rabbits after 4 weeks of feeding with control or low-K^+ diet. Serum $[K^+]$ in all low-K^+ diet rabbits after 4 weeks was less than 3.0 mM (2.40 ± 0.14 mM; $n = 9$). The action potentials were recorded at room temperature with solutions similar to the standard 135 mM K^+ pipette solution and 5 mM K^+ bath solution (see Methods and Supplemental Table 1). Action potential duration at 90% repolarization

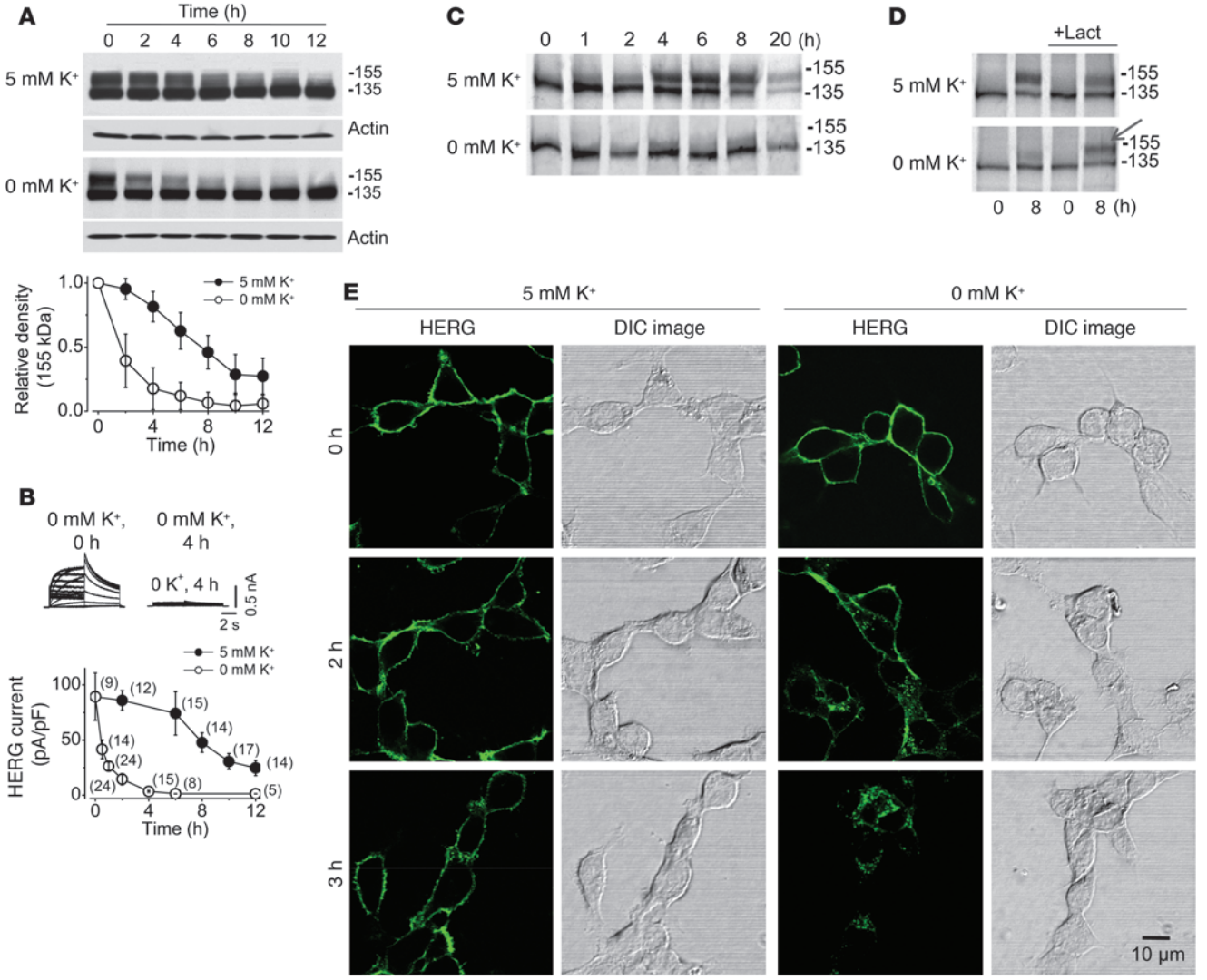

Figure 4

Accelerated internalization and degradation of cell surface HERG protein is responsible for 0 mM K^+_o–induced I_{HERG} reduction. (**A** and **B**) Time-dependent effects of incubating HERG-HEK cells with BFA (10 μM) in 0 or 5 mM K^+ MEM on HERG protein expression level (**A**) or I_{HERG} amplitude (**B**). (**A**) The 155-kDa band intensities in 0 or 5 mM K^+ MEM at each time point were normalized to their initial values and plotted against time ($n = 5$). (**B**) HERG tail current upon repolarization to –50 mV after a 50-mV depolarization was measured and normalized to control value (time 0). The HERG currents shown in the inset were recorded using the protocol shown in Figure 1A. (**C**) Pulse-chase analysis of HERG trafficking in 0 or 5 mM K^+ MEM. (**D**) Pulse-chase analysis of HERG trafficking in 0 or 5 mM K^+ MEM with or without 20 μM lactacystin (Lact). The mature 155-kDa HERG channel protein is denoted by an arrow. (**E**) Time-dependent internalization of the surface HERG channels (green) labeled using an anti-HERG antibody. The cells were shown using DIC images. Similar results were observed in each set of 8 independent experiments. Scale bar: 10 μm. Numbers in parentheses denote *n* from at least 3 independent experiments.

(APD_{90}) was significantly prolonged in cardiomyocytes from rabbits fed the low-K^+ diet compared with those from control rabbits (Figure 2C). The resting membrane potentials of ventricular myocytes were not different between control and low-K^+ groups (control, 77.8 ± 0.7 mV, $n = 14$; low K^+, 75.4 ± 1.0 mV, $n = 14$; $P > 0.05$). The L-type Ca^{2+} current (Ba^{2+} used as a charge carrier; Figure 2D) and the inwardly rectifying K^+ current (I_{K1}; Figure 2E) from hypokalemic rabbit ventricular myocytes were not different from those of control rabbits. While the transient outward K^+ current slightly increased and the slowly activating delayed rectifier K^+ current slightly decreased in hypokalemic rabbit ventricular myocytes, these changes did not reach statistical significance compared with those in control rabbits (Supplemental Figure 2). To evaluate I_{Kr}, we use the amplitude of the tail current recorded with the standard 5 mM K^+ bath and 135 mM K^+ pipette solutions upon repolarization to –50 mV after a depolarization to +50 mV (14). I_{Kr} was significantly reduced in hypokalemic rabbit ventricular myocytes (Figure 2F). Because I_{Kr} recorded using this conventional method is small and contaminated by other currents, we isolated pure I_{Kr} in ventricular myocytes using Cs^+ as the charge carrier in order to confirm the reduction of I_{Kr}. We previously demonstrated that both HERG channels expressed in HEK cells and native I_{Kr} in rab-

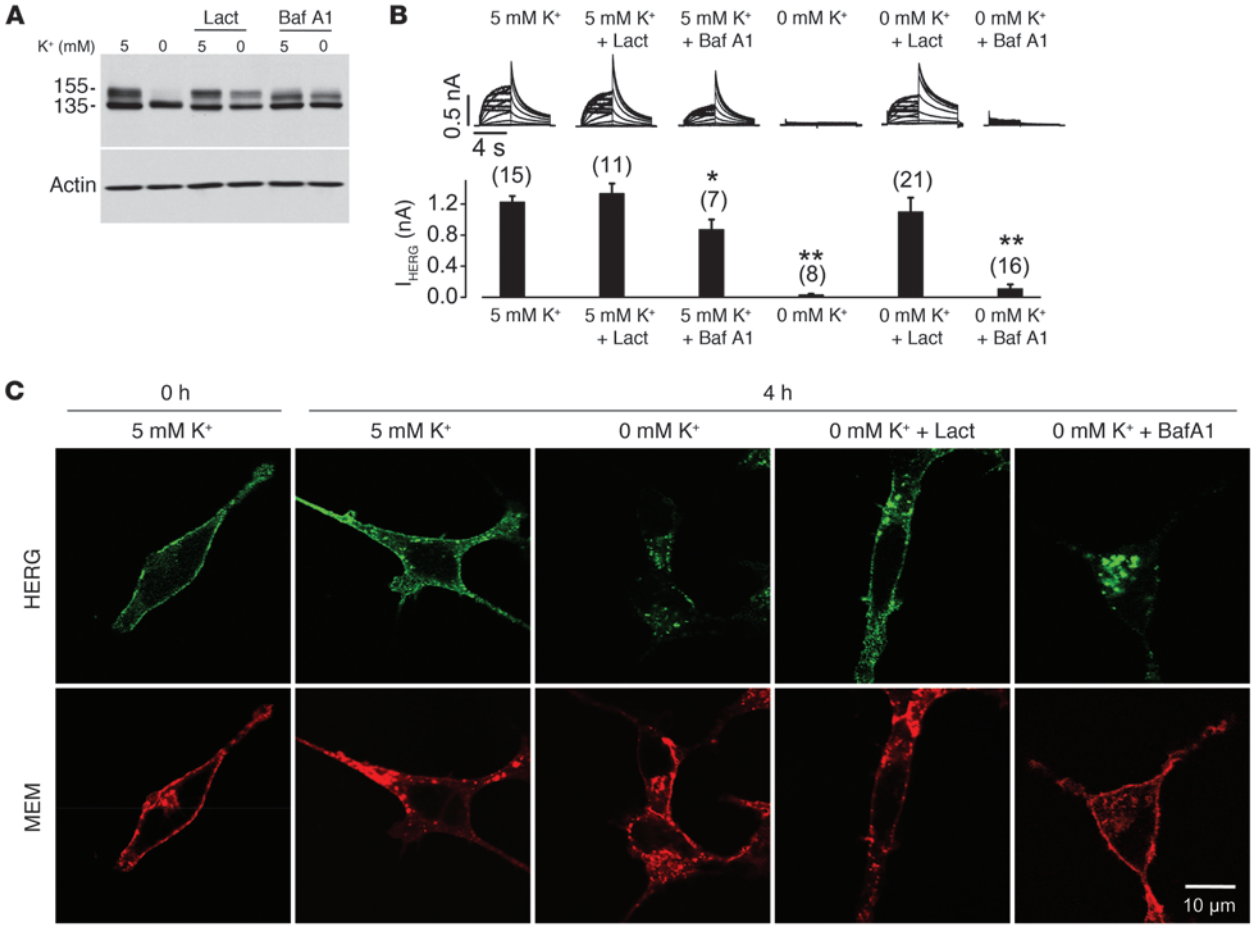

Figure 5

Effects of proteasomal or lysosomal inhibition on 0 mM K^+ exposure-induced HERG internalization. (**A**) Effects of lactacystin and bafilomycin A1 (Baf A1) on 0 mM K^+ exposure-induced reduction of the 155-kDa HERG protein. Proteins were extracted from HERG-HEK cells cultured in 5 or 0 mM K^+ MEM alone or with 20 μM lactacystin or 1 μM bafilomycin A1 for 6 hours. HERG expression levels under various conditions are shown (n = 6). (**B**) Effects of lactacystin or bafilomycin A1 on 0 mM K^+–induced reduction of I_{HERG}. Families of I_{HERG} were recorded using the protocol shown in Figure 1A. The HERG-HEK cells were cultured in 0 or 5 mM K^+ MEM in the absence or presence of lactacystin (20 μM) or bafilomycin A1 (1 μM) for 4 hours. Cells were then collected in drug-free 5 mM K^+ MEM, and I_{HERG} was recorded using the whole-cell clamp method in 5 mM K^+ bath solution. Tail current at –50 mV after a 50-mV depolarization was used to measure the HERG current amplitude. Currents in each condition were compared with the current from cells in 5 mM K^+. *P < 0.05, **P < 0.01 versus 5 mM K^+. (**C**) Localization of surface-labeled HERG channels after culture under various conditions. The cell surface HERG was labeled using an anti-HERG antibody. Cells were cultured in different conditions and then permeabilized. The labeled HERG was detected using an Alexa Fluor 488–conjugated (green) secondary antibody. The cell membrane was labeled using an Alexa Fluor 594–conjugated (red) WGA. Scale bar: 10 μm. Numbers in parentheses denote n from at least 3 independent experiments.

bit ventricular myocytes display a unique Cs^+ permeation property, and because Cs^+ blocks other cardiac K^+ channels, recording Cs^+-carried I_{Kr} using symmetrical Cs^+ solutions represents an effective means of obtaining pure I_{Kr} and is especially useful for analyzing I_{Kr} density (13, 15). The magnitude of the Cs^+-mediated I_{Kr} in ventricular myocytes from hypokalemic rabbits was significantly smaller than that from control rabbits (Figure 2G). Furthermore, the expression level of the mature form of I_{Kr} protein (155-kDa band) in rabbits on the low-K^+ diet was much lower than that in control rabbits (Figure 2H). Thus, like HERG channels, native I_{Kr} also requires K^+_o for proper plasma membrane expression.

Lowering $[K^+]_o$ accelerates HERG internalization and degradation. We determined the effects of $[K^+]_o$ on plasma membrane HERG expression levels in the HERG-HEK cell line. The HERG proteins extracted from cells cultured in normal 5 mM K^+ MEM displayed 2 bands with molecular masses of 155 and 135 kDa (Figure 3A), representing the mature fully glycosylated form in the plasma membrane (155 kDa) and the immature core-glycosylated form residing in the ER (135 kDa) (13, 16). Overnight culture of HERG-HEK cells in various $[K^+]_o$ did not alter the expression level of the 135-kDa band, but produced a K^+-dependent reduction in the expression level of the 155-kDa band, with an EC_{50} of 0.41 ± 0.05 mM (H, 4.1; n = 4; Figure 3B). The 155-kDa band is located in the plasma membrane, as it can be completely digested by the external proteinase K (13). When the cell surface protein was isolated using a membrane protein biotinylation kit, the density of the 155-kDa HERG band in cells under 0 mM K^+ MEM culture for 12 hours decreased by 81.8% ± 3.5% compared with that in cells under 5 mM

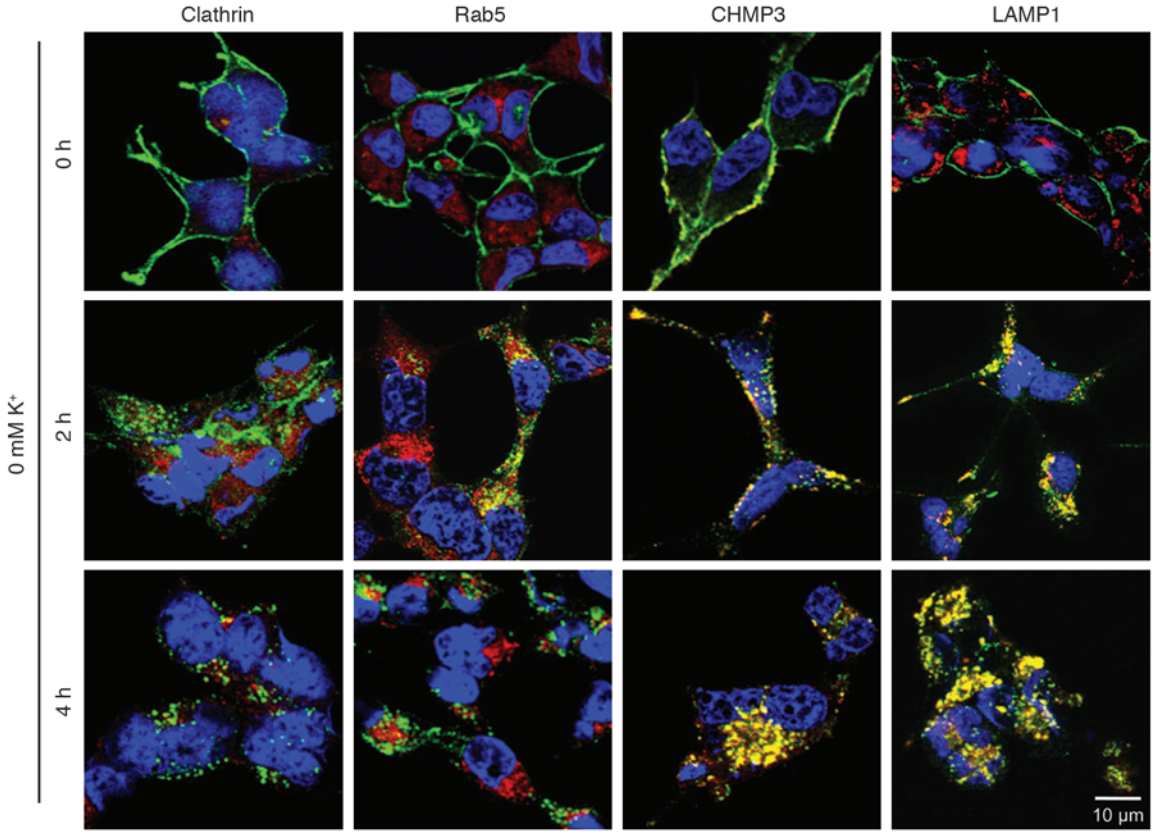

Figure 6
Localization of HERG channels with endocytic degradation pathway markers clathrin, Rab5, CHMP3, or LAMP1 during internalization in 0 mM K^+. Cell surface HERG channels were labeled by treating live HERG-HEK cells in culture with an anti-HERG antibody. Before (0 hours) and after exposure to 0 mM K^+ for 2 or 4 hours, the cells were fixed and permeabilized. An Alexa Fluor 488–cojugated (green) secondary antibody was used to stain HERG channels. Various primary and Alexa Fluor 546–conjugated (red) secondary antibodies were used to stain clathrin, Rab5, CHMP3, and LAMP1. Scale bar: 10 μm.

K^+ MEM culture (n = 3; P < 0.01; Figure 3C). Thus, the decrease in cell surface expression level of HERG channels underlies the low K^+_o–induced I_{HERG} reduction.

We examined the time courses of 0 mM K^+–induced reduction of I_{HERG} and the 155-kDa HERG expression levels. I_{HERG} and the 155-kDa band were stable in 5 mM K^+ MEM (Figure 3, D and E). However, I_{HERG} was reduced by 88% ± 2% after 6 hours and by 96% ± 2% after 12 hours of exposure to 0 mM K^+ MEM (Figure 3D). The reduction of the 155-kDa band followed a time course that closely paralleled the time course of I_{HERG} reduction (n = 4; Figure 3E).

The cell surface density of HERG channels reflects the equilibrium between its maturation and degradation. To investigate the mechanism of the 0 mM K^+_o–induced reduction of the 155-kDa HERG protein, we blocked forward trafficking with the Golgi transit inhibitor brefeldin A (BFA). BFA is a fungal antibiotic that inhibits protein transport from the ER to the Golgi. The HERG-HEK cells were pretreated with BFA (10 μM) in normal MEM for 1 hour and then cultured in 0 or 5 mM K^+ MEM in the continued presence of BFA. BFA blocked the conversion of HERG from its immature 135-kDa form into its mature 155-kDa form (Figure 4A). As a result of the blockade of protein forward trafficking, the decrease in the 155-kDa band should represent solely the rate of degradation of preexisting mature channels. As shown in Figure 4A, when cells were incubated in 5 mM K^+ MEM with BFA, the 155-kDa band decreased by about half (54% ± 13%; n = 5) in 8 hours. In contrast, incubation of the cells in 0 mM K^+ MEM with BFA resulted in a much faster decrease in the 155-kDa band, reduced by more than half (61% ± 21%; n = 5) in 2 hours. Similarly, in 5 mM K^+ with BFA, I_{HERG} decreased by 42% ± 2% in 8 hours, and in 0 mM K^+ with BFA, I_{HERG} decreased by 82% ± 8% in 2 hours (Figure 4B). These results indicate that low $[K^+]_o$ greatly accelerated degradation of the 155-kDa form of HERG protein that underlies the HERG current.

We then examined whether chronic exposure to low $[K^+]_o$ impairs HERG forward trafficking by performing pulse-chase experiments using metabolic pulse labeling. The labeled HERG proteins were chased in cells cultured in 0 or 5 mM K^+ for up to 20 hours. In 5 mM K^+, the [^{35}S]-labeled HERG protein initially appeared as a 135-kDa HERG band, and the 155-kDa HERG band gradually intensified with time (Figure 4C), indicating a precursor-product relationship between the 135- and 155-kDa bands (17). In 0 mM K^+ MEM, the [^{35}S]-labeled HERG protein was also initially synthesized as the 135-kDa band. However, the 155-kDa band was barely detected during 1–20 hours of chase (Figure 4C). We showed that the 155-kDa form of HERG degraded faster in 0 mM K^+ (Figure 4A). To examine whether the absence of 155-kDa form was caused by the fast degradation, we

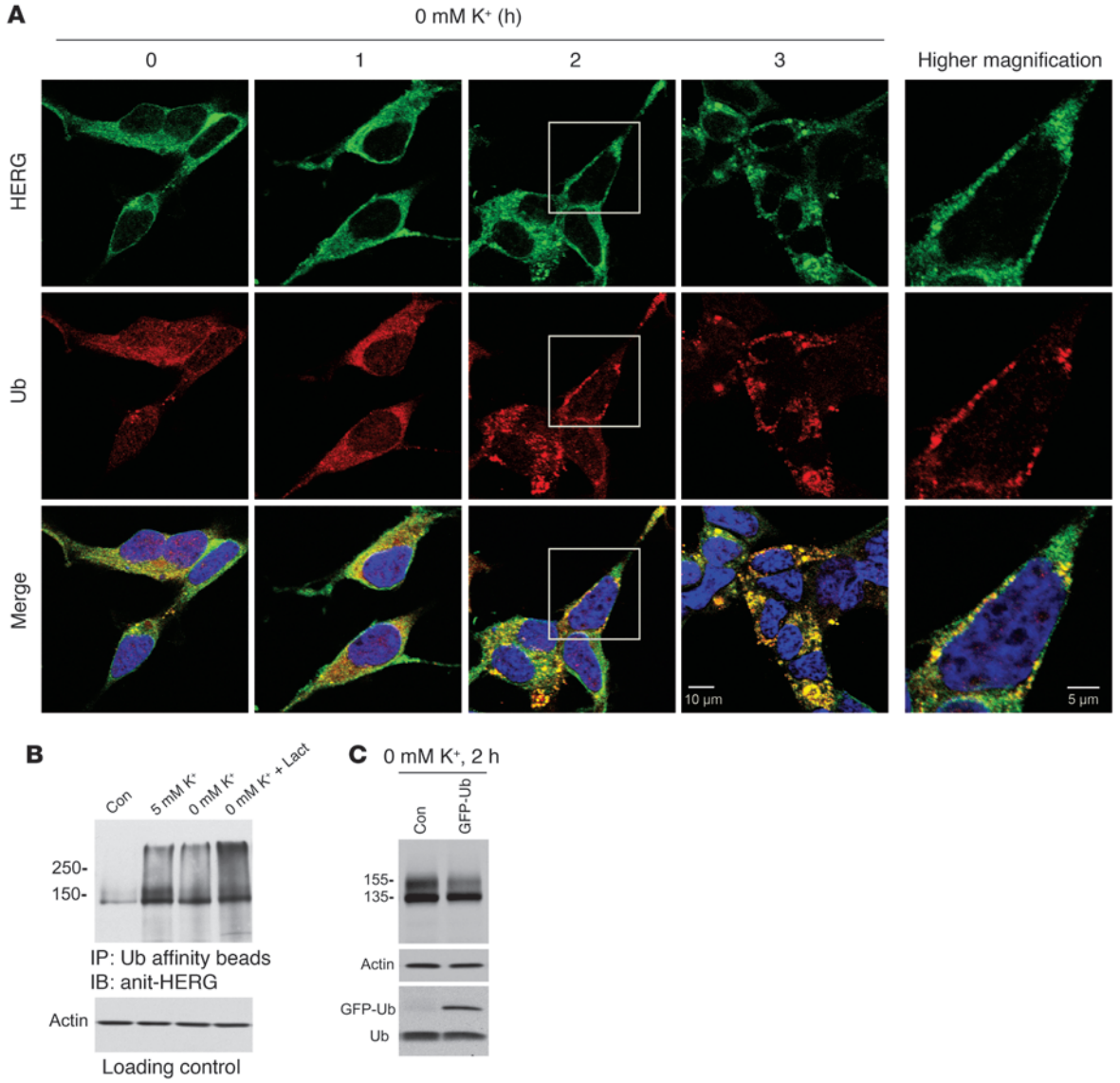

Figure 7

Involvement of ubiquitination in HERG degradation in 0 mM K^+. (**A**) Colocalization between HERG and Ub. HERG-HEK cells were cultured in 0 mM K^+ MEM for varying periods of time and then fixed and permeabilized. Cells were stained with an anti-Ub primary antibody and an Alexa Fluor 546–conjugated (red) secondary antibody. HERG channels were stained with an anti-HERG antibody and an Alexa Fluor 488–conjugated (green) secondary antibody. Higher-magnification views of the boxed areas in the 2-hour panels are shown at right. Scale bars: 10 μm (left panels); 5 μm (magnified boxed regions). (**B**) Ubiquitinated proteins were precipitated using Ub affinity beads from 0.5-mg lysates from cells subjected to the indicated culture conditions for 6 hours. The ubiquitinated HERG was detected using an anti-HERG antibody ($n = 7$). To ensure equal cell lysates in each condition, 15 μl protein mixture of each sample was loaded in a gel before immunoprecipitation, and actin expression level was measured and used for loading control. (**C**) Effects of overexpression of GFP-Ub on HERG expression in HERG-HEK cells after 2 hours' exposure to 0 mM K^+ ($n = 5$). A higher–molecular mass band corresponding to free monomeric GFP-Ub was detected only in GFP-Ub–transfected HERG-HEK cells, whereas the 8.5-kDa free Ub bands were detected in both GFP-Ub–transfected and nontransfected HERG-HEK cells.

performed pulse-chase experiments in the presence of lactacystin, which prevents proteasome-mediated protein degradation and membrane protein internalization (17–22). Lactacystin treatment revealed expression of the 155-kDa HERG band in 0 mM K^+ (Figure 4D), indicating that under 0 mM K^+ conditions, the 135-kDa form of HERG indeed matured into the 155-kDa form, and that in the absence of lactacystin, the mature form degraded quickly and thus failed to accumulate. To address whether exposing cells to 0 mM K^+ MEM changes the intracellular environment and causes the observed decrease in 155-kDa HERG expression, we measured intracellular pH using a Cytomics FC 500 flow cytometer with the pH-sensitive dye SNARF-1 and intracellular free Ca^{2+} concentration using an InCyt dual-wavelength imaging system (Supplemental Methods). Exposure to 0 mM K^+ MEM for 6 hours did not change the intracellular pH or free Ca^{2+} concentrations of HERG-HEK cells (Supplemental Figure 3). These

results suggest that 0 mM K^+–induced reduction of the 155-kDa form of HERG channels may not be caused by disruptive forward trafficking, but may be caused by destabilization and degradation of the membrane HERG channels.

To visualize the fate of plasma membrane HERG channels in low K^+, we labeled cell surface HERG protein with an anti-HERG antibody that targets the S1–S2 external linker region of the HERG channel. We incubated HERG-HEK cells for 30 minutes at room temperature with the anti-HERG antibody. Unbound antibody was then completely washed away, and the cells were cultured in 0 or 5 mM K^+ MEM. The cells were then fixed at different time points, and the localization of labeled HERG was visualized by incubating the permeabilized cells with Alexa Fluor 488–conjugated secondary antibody. At the 0 time point, the labeled HERG was localized in the plasma membrane. In 5 mM K^+ MEM culture, the majority of the labeled HERG channels remained in the plasma membrane during 3 hours of culture. However, in 0 mM K^+ MEM culture, the labeled HERG channels displayed time-dependent internalization and were completely internalized in 3 hours (Figure 4E).

To investigate the cellular machinery underling HERG internalization and degradation in 0 mM K^+, we examined the effects of proteasomal and lysosomal inhibitors on the 0 mM K^+–induced 155-kDa HERG reduction. The proteasomal inhibitor lactacystin and the lysosomal inhibitor bafilomycin A1 were used, both of which impeded 0 mM K^+–induced reduction of the 155-kDa HERG band (Figure 5A). To determine the function of the preserved 155-kDa HERG in 0 mM K^+, we recorded I_{HERG} using the whole-cell patch-clamp method. Despite the preserved 155-kDa HERG bands in Western blot analysis (Figure 5A), lactacystin-treated cells, but not bafilomycin A1–treated cells, displayed I_{HERG} (Figure 5B). The absence of I_{HERG} in cells cultured in 0 mM K^+ with bafilomycin A1 was not caused by bafilomycin A1, because cells treated with bafilomycin A1 in 5 mM K^+ displayed current that was robust, albeit smaller than that of cells in 5 mM K^+ without drug (Figure 5B). To determine the underlying mechanisms for the different effects of these 2 agents on I_{HERG}, we examined HERG protein localization using confocal microscopy. As shown in Figure 5C, while the 0 mM K^+–induced HERG internalization was markedly prevented by lactacystin, it was not prevented by bafilomycin A1. Instead, bafilomycin A1 treatment led to accumulation of internalized HERG channels inside the cell under 0 mM K^+ conditions (Figure 5C). This result is in contrast to the prior demonstration that under normal culture conditions, the 155-kDa band represents the functional channels located on the cell surface, as it can be completely digested by externally applied proteinase K (13, 23). The presence of the 155-kDa band in 0 mM K^+ with bafilomycin A1 indicates that we have captured the recently internalized pool of surface channels for the first time, and that the presence of the upper band in this case does not represent the functional surface channels as seen under normal culture conditions.

To determine the HERG endocytic routes and localization of the internalized HERG channels from the cell surface, we labeled cell surface HERG with an anti-HERG antibody, followed the fate of labeled HERG channels at various time points, and examined HERG colocalization with known endocytic markers. After labeling of the surface HERG channels, cells cultured in 0 mM K^+ MEM for various periods of time were fixed and permeabilized. The labeled HERG was detected with Alexa Fluor 488–conjugated secondary antibody. Specific marker proteins of the endocytic routes were stained with appropriate primary and secondary antibodies, and their colocalization with HERG channels was examined. When HERG-HEK cells were exposed to 0 mM K^+ MEM, HERG internalization became obvious at 3 hours (Figure 4E). Therefore, we examined HERG colocalization with various endocytic marker proteins at 2 and 4 hours after the HERG-HEK cells were exposed to 0 mM K^+ MEM. First, we examined the colocalization of HERG and clathrin because clathrin plays a key role in the classical clathrin-mediated endocytosis of membrane proteins. Our data showed that HERG channels did not colocalize with clathrin at any time point examined (Figure 6). In addition, as shown in Supplemental Figure 4, knockdown of clathrin using clathrin siRNA transfection did not affect 0 mM K^+–induced reduction of the 155-kDa HERG band. These results suggest that the classical clathrin-mediated endocytic pathway may not be the route for HERG internalization. Second, we examined the colocalization between HERG and an early endosome marker, Rab5, and found partial colocalization at 2 hours after exposure of cells to 0 mM K^+ MEM (Figure 6). However, internalized HERG channels were not colocalized with Rab5 at 4 hours after exposure to 0 mM K^+, when internalization of labeled HERG was complete. These data suggest that internalized HERG channels transit through early endosomes on their way to sorting and degradation. Third, we examined HERG colocalization with multivesicular bodies (MVBs). Endosomal sorting complexes required for transport (ESCRT) represent important machinery for sorting ubiquitinated cargo into luminal vesicles of MVBs, which fuse directly with lysosomes, the terminal compartment of the endocytic pathway (24). We used the charged multivesicular body protein 3 (CHMP3) as a MVB marker. CHMP3 displays predominantly plasma membrane and vesicular localization and is important for MVB formation and protein sorting (25). HERG channels were colocalized with MVBs at both 2 and 4 hours after exposure to 0 mM K^+ (Figure 6). Finally, we used lysosomal-associated membrane protein 1 (LAMP1) as a lysosome marker and examined whether HERG is localized in lysosomes. HERG was colocalized with LAMP1 partially at 2 hours — and colocalization substantially increased at 4 hours — after exposure of cells to 0 mM K^+ MEM (Figure 6). Overall, these results indicate that under low-K^+ conditions, HERG channels transit through endosomes into the MVBs, which further fuse with lysosome for degradation.

Many membrane proteins that are degraded in the lysosomes are sorted through the MVB pathway. Significantly, attachment of a single ubiquitin (Ub) is required and sufficient to trigger target proteins to enter into MVBs for degradation (26). In addition, substrate proteins are known to be tagged by polyubiquitin chains as a signal for proteasomal degradation (27). To determine the interactions between HERG and Ub during the endocytic route of HERG internalization, we examined the colocalization between HERG and Ub in HERG-HEK cells. Cells were exposed to 0 mM K^+ MEM for 1, 2, or 3 hours and then fixed and permeabilized. Ub and HERG were labeled with appropriate primary and secondary antibodies. As shown in Figure 7A, under control conditions, HERG channels were localized throughout the cell and concentrated in the plasma membrane. Ub was evenly distributed throughout the cell. At 1 hour after exposure to 0 mM K^+ MEM, internalization of HERG channels was not yet obvious, and localization of both HERG and Ub was similar to that in the control. At 2 hours after exposure to 0 mM K^+ MEM, HERG channels clustered around the plasma membrane with substantial punctate staining, which suggests that HERG channels aggregated prior to internalization. Remarkably, Ub followed a similar pattern of cellular distribution, displaying

a colocalization pattern with HERG. At 3 hours after exposure to 0 mM K^+ MEM, HERG channels were essentially internalized and displayed punctate intracellular localization. Again, Ub displayed the same pattern of intracellular localization and was colocalized with HERG. These results indicate that ubiquitination of HERG channels triggers HERG internalization in low-K^+ conditions. We further confirmed the Ub-HERG interactions using Western blot analysis. Ubiquitination of HERG proteins was analyzed from HERG-HEK cells cultured in 0 or 5 mM K^+ alone, or in 0 mM K^+ plus lactacystin (20 μM), for 6 hours. Ubiquitinated proteins were isolated using Ub affinity beads from whole-cell lysates, and the ubiquitinated HERG protein levels were detected using an anti-HERG antibody. As shown in Figure 7B, ubiquitinated HERG channels were detected in cells cultured in both 0 and 5 mM K^+ MEM for 6 hours. A slight lower expression level of ubiquitinated HERG channels observed in 0 mM K^+ was consistent with accelerated HERG degradation under this condition. Importantly, incubation with lactacystin caused significant accumulation of ubiquitinated HERG channels in 0 mM K^+ (Figure 7B), indicating that HERG channels are ubiquitinated during 0 mM K^+–induced degradation. To directly examine the role of Ub in HERG degradation in 0 mM K^+, we overexpressed GFP-tagged Ub (GFP-Ub) in HERG-HEK cells. At 36 hours after transfection, we exposed the GFP-Ub–transfected cells to 0 mM K^+ for 2 hours and examined HERG expression levels. Overexpression of GFP-Ub markedly promoted 0 mM K^+–induced reduction of the 155-kDa HERG band. After 2 hours of exposure to 0 mM K^+, a substantial amount of the 155-kDa form remained in HERG-HEK cells, while it markedly decreased in the GFP-Ub–transfected HERG-HEK cells (Figure 7C). Notably, Ub overexpression preferentially reduced the expression levels of the 155-kDa membrane HERG in 0 mM K^+, as expression levels of the 135-kDa ER form of HERG and actin were minimally affected (Figure 7C). This result further supports the notion that ubiquitination triggers HERG internalization under low-K^+ conditions.

Discussion

Our present results demonstrate, for the first time to our knowledge, that the plasma membrane density of the voltage-gated K^+ channel HERG is strictly controlled by a physiological factor, $[K^+]_o$. We have illustrated that HERG required K^+_o for its membrane stability. Under low-K^+ conditions, HERG channels in the plasma membrane were internalized and degraded. For a single HERG channel, the equilibrium between K^+ bound and unbound state was $[K^+]_o$ dependent. When $[K^+]_o$ decreased, the likelihood for a channel residing in a non-K^+ bound state increased. Thus, the membrane density of HERG is controlled by $[K^+]_o$.

Hypokalemia is an important clinical risk factor for LQTS. Cardiac action potentials in vitro are shorter at higher $[K^+]_o$ and longer at lower $[K^+]_o$ (9). We showed that hypokalemic rabbits displayed a prolonged QT interval and that ventricular myocytes isolated from hypokalemic rabbits displayed a prolonged APD_{90} (Figure 2C). The effects of low $[K^+]_o$ on APD_{90} was previously linked to the acute effects of K^+_o on I_{HERG}/I_{Kr}: it was reported that a reduction in $[K^+]_o$ decreased I_{HERG}/I_{Kr}, because of either enhanced inactivation (28) or increased inhibition by Na^+, as K^+_o competes with Na^+ for binding to the HERG external pore mouth (29). Our present findings demonstrate a mechanism that we believe to be new: $[K^+]_o$ strictly controls the density of HERG channels in the cell plasma membrane. We showed that when steady-state alterations of I_{HERG} at a changed $[K^+]_o$ were achieved, K^+_o regulated the HERG current with an EC_{50} of 2.1 mM (Figure 1D). The serum $[K^+]$ in rabbits after 4 weeks on a low-K^+ diet decreased by approximately 50% compared with the control rabbits (low K^+, 2.4 mM; control, 4.69 mM), and the hypokalemic rabbits displayed a prolonged QT interval (low K^+, 0.36 seconds; control, 0.27 seconds). Hypokalemia is defined as a serum K^+ level less than 3.5 mM (30), and the condition has been associated with the occurrence of cardiac arrhythmic events such as Torsades de pointes (30–32). In hypokalemic patients, serum $[K^+]$ of 2.1 and 2.8 mM were reported (31). In a profoundly hypokalemic patient, a serum $[K^+]$ of 1.2 mM was associated with pulseless ventricular tachycardia, and the patient was successfully resuscitated by K^+ supplementation (30). Our conclusion that K^+_o controls HERG membrane density provides a potential clinically relevant mechanistic link between hypokalemia and LQTS.

In inherited LQT2, a large group of mutations produce trafficking-deficient HERG channels that are retained in the ER by quality control mechanisms (5). Additionally, some drugs disrupt HERG forward trafficking, thereby causing LQTS (13, 33, 34). Recently, Wang et al. found that inhibition of Na^+/K^+ ATPase disrupted HERG forward trafficking (34, 35). However, the 0 mM K^+–induced reduction of 155-kDa HERG expression levels is most likely due to the increased membrane instability and degradation of HERG channels, not to the impaired forward trafficking. We demonstrated that the 135-kDa form of HERG indeed matured into the 155-kDa form under 0 mM K^+ culture conditions, when protein degradation was inhibited (Figure 4D). To directly address the role of impaired forward trafficking in the process of 0 mM K^+–induced HERG reduction, we showed that when forward protein trafficking was blocked by BFA in 5 mM K^+ MEM, I_{HERG} was reduced by 17.1% in 6 hours (Figure 4B). This result is consistent with a prior report that the mature 155-kDa HERG channel protein decays with a half-life of about 11 hours (36). On the other hand, I_{HERG} and the 155-kDa band were reduced by more than 80% in 6 hours in 0 mM K^+ MEM (Figure 3, D and E). Furthermore, by labeling the cell surface HERG channels and following their fate in 0 mM K^+ MEM, we demonstrated that the surface HERG channels were internalized and degraded within 4 hours under 0 mM K^+ MEM culture conditions (Figures 4–7). Thus, unstable membrane localization and accelerated degradation is responsible for 0 mM K^+–induced reduction of functional HERG channels. The destabilizing effect of low K^+ could cause a conformational change that exposes Ub signal sites and triggers internalization. The Ub tag is well known to trigger internalization and degradation of various membrane proteins (19, 20, 26, 37–39).

The 2 major cellular pathways for protein degradation are the proteasomal and lysosomal pathways. Polyubiquitination is usually the sorting signal for the proteasomal degradation route and is responsible for degradation of cytosolic proteins and those destined for ER-associated degradation (27). On the other hand, monoubiquitination triggers the sorting of membrane proteins into luminal vesicles of MVBs and subsequent delivery to lysosomes for degradation (38). Once protein cargo is tagged by Ub, it is recognized and sorted by the ESCRT complex (38, 39). Our data showed that HERG and Ub shared the same dynamic distribution pattern and were colocalized during HERG internalization (Figure 7A), that HERG channels underwent Ub modification (Figure 7B), and that internalized HERG channels colocalized with MVBs and lysosomes under low-K^+ conditions (Figure 6). These results indicate that the ubiquitination/MVB/lysosome pathway is responsible for HERG degradation in low $[K^+]$.

In addition to being responsible for degradation of cytosolic proteins, proteasomal activity is required for the internalization of many membrane proteins, such as glutamate receptors (20), tropomyosin-regulated kinase A receptor (22), growth hormone receptor (19), chloride channel CFTR (21), and the gap junction channel connexin43 (18). We demonstrated that proteasomal inhibition also impeded low K^+–induced HERG internalization (Figure 5). There are a number of potential interpretations for this result. First, prolonged proteasomal inhibition may cause accumulation of ubiquitinated proteins and depletion of the free Ub pool (27). Second, internalization of membrane proteins is a complex dynamic process that may depend on proteasomal activity (26, 38, 39). For example, proteasomal activity is required for the sorting of ubiquitinated cargo proteins in MVBs (26). In the presence of proteasomal inhibitors, the impairment of HERG sorting in the early stage of degradation may lead to a larger pool of internalized HERG available for export to the surface, thus masking the induction of internalization by low K^+. Indeed, the results of our pulse-chase experiment with lactacystin directly supports this conclusion.

The electrical activities generated by ion channels are essential for a wide variety of physiological processes (40). Although internalization represents an important mechanism for regulation of various receptors in the cell membrane (19, 20, 26, 37), information on the membrane stability of WT ion channels is limited, and few manipulations are available for regulating the functional expression of ion channels. Our finding — which we believe to be novel — that K^+_o dictates the plasma membrane density of voltage-gated channel HERG surface expression via controlling channel internalization and degradation represents a means by which HERG function is regulated.

Methods

Molecular biology and electrophysiological recordings. Procedures for transfection and electrophysiological recordings were performed as previously described (13, 15). Stable cell lines expressing various K^+ channels were generated using G418 for selection. The HERG stable cell line was provided by C. January (University of Wisconsin, Madison, Wisconsin, USA). A custom 0 mM K^+ MEM (Millipore) was used as a baseline medium, and KCl was added to make the desired $[K^+]$ of MEM. For whole-cell clamp recordings, the standard 135-mM K^+ pipette solution contained 135 mM KCl, 5 mM EGTA, 1 mM $MgCl_2$, and 10 mM HEPES (pH 7.2). The standard 5-mM K^+ bath solution contained 135 mM NaCl, 5 mM KCl, 2 mM $CaCl_2$, 1 mM $MgCl_2$, 10 mM glucose, and 10 mM HEPES (pH 7.4). To assess the $[K^+]_o$ dependence of I_{HERG}, tail current amplitudes were fitted to the Hill equation: $I_{HERG} = 1 - 1/[1 + (D/EC_{50})^H]$, where D is the $[K^+]_o$, EC_{50} is the $[K^+]_o$ concentration for 50% maximal conductance, and H is the Hill coefficient. All patch-clamp experiments were performed at room temperature (22 ± 1°C).

Animal experiments. Experimental protocols used for animal studies were approved by the Queen's University and University of Manitoba Animal Care Committees. For the hypokalemia rabbit model, New Zealand white rabbits (2.5–3.0 kg) were divided into 2 groups and were fed a normal or a low-K^+ diet, both from TestDiet. Blood was taken weekly to monitor liver (e.g., AST, ALT, and A/G ratio) and kidney (e.g., urea and creatinine) function as well as electrolyte levels, including K^+ (MAFRI Vet Lab). ECG recordings were taken on lightly anesthetized rabbits using a BioPac MP100 system. The ECG signal was analyzed using Acqknowledge 3.7.3 software (Biopac Systems Inc.).

Cardiomyocytes were isolated from rabbits fed control or low-K^+ diet after 4 weeks. Hearts were excised from anesthetized rabbits, mounted on a Langendorff apparatus, and flushed at 20 ml/min with Ca^{2+}-free Kreb's solution (110.0 mM NaCl, 2.6 mM KCl, 1.2 mM KH_2PO_4, 1.2 mM $MgSO_4$, 25.0 mM $NaHCO_3$, 11.0 mM glucose, 15.0 mM HEPES, and 0.5% BSA; pH 7.2). The hearts were then perfused with Kreb's solution plus collagenase II (295 U/ml; Worthington). Tissue biopsies were taken from the left ventricle at different time points between 35 and 50 minutes and minced in KB solution (10.0 mM KCl, 120.0 mM K-glutamate, 10.0 mM KH_2PO_4, 1.8 mM $MgSO_4$, 10.0 mM taurine, 10.0 mM HEPES, 0.5 mM EGTA, 20.0 mM glucose, and 10.0 mM mannitol; pH 7.3) to obtain optimal isolated myocytes. Cells were filtered through cheesecloth and kept in 1% BSA-containing KB solution at room temperature for electrophysiology studies.

For action potential and ionic current recordings from rabbit ventricular myocytes, whole-cell patch-clamp method was used (13). Action potentials and ionic currents were acquired and analyzed using pClamp 10 software (Molecular Devices). The compositions of pipette and bath solutions for recording action potentials and some of the ionic currents were reported previously (13); a complete list is provided in Supplemental Table 1. Action potentials were recorded in current clamp mode (13), elicited by injecting currents of 3-ms duration with amplitude 1.2 times the threshold through the recording electrode. Cells were stimulated at 0.2 Hz. Patch-clamp experiments were performed at room temperature (22 ± 1°C).

Western blot analysis. Whole cell lysates from HERG-expressing HEK 293 cells were used for Western blot analysis. For HERG detection, proteins were separated on 7.0% SDS polyacrylamide gels and electroblotted overnight at 4°C on polyvinylidene difluoride (PVDF) membrane. The membrane was then blocked using 5% nonfat dry milk and 0.1% Tween 20 in Tris-buffered saline and immunoblotted for 1 hour with a rabbit anti-Kv11.1 primary antibody (Sigma-Aldrich). HERG signals were detected using goat anti-rabbit horseradish peroxidase–conjugated secondary antibody and ECL detection kit (GE Healthcare). Cell surface proteins were isolated using a biotinylation kit (Cell Surface Protein Isolation Kit; Pierce). An Ubiquitin Protein Enrichment Kit (Calbiochem) was used to isolate ubiquitinated proteins. Cell membrane protein extraction from rabbit hearts was performed in a cold room (4°C). Left ventricular tissue was homogenized using a Pro 250 homogenizer (DiaMed Lab Supplies Inc.). The homogenization buffer contained 10 mM $NaHCO_3$, 5 mM NaN_3, 15 mM Tris-HCl (pH 6.8), and protease inhibitors leupeptin (1 μM), pepstatin (1 μM), and phenylmethylsulfonyl fluoride (100 μM). The homogenate was centrifuged for 20 minutes at 10,000 *g* (JA 20.0 rotor; Beckman). The supernatant was collected and centrifuged for 45 minutes at 40,000 *g* (JA 20.0 rotor; Beckman). The pellet was suspended in a buffer containing 0.6 M KCl and 20 mM Tris-HCl (pH 6.8) and recentrifuged for 45 minutes at 40,000 *g*. The final pellet was suspended in a buffer containing 0.25 M sucrose and 10 mM histidine (pH 7.0) and stored at –86°C. Extracted proteins were separated on 7.0% SDS polyacrylamide gels and electroblotted overnight at 4°C on PVDF membrane. A goat anti-HERG antibody (C-20; Santa Cruz Biotechnology Inc.) and an anti-goat secondary antibody conjugated to horseradish peroxidase were used for I_{Kr} detection using an ECL Plus Western Blotting Detection System (GE Healthcare).

Pulse-chase experiments. For metabolic labeling and immunoprecipitation, HERG-HEK cells in 60-mm plates were incubated with MEM for 12 hours. The intracellular pools of methionine and cysteine were depleted by incubating cells for 30 minutes in methionine- and cysteine-free DMEM. Cells were pulse-labeled for 45 minutes in methionine- and cysteine-free medium containing 110 μCi/ml [^{35}S]methionine/cysteine. After pulse labeling, HERG-HEK cells were chased in 0 or 5 mM K^+ MEM supplemented with 2 mM unlabeled methionine and cysteine for time intervals up to 20 hours. At each chase period, cells were lysed, and proteins were immunoprecipitated with HERG antibody (N20; Santa Cruz Biotechnology Inc.), subjected to 7% SDS-PAGE, and visualized with autoradiography.

Immunofluorescence microscopy. Cells grown on cover glasses were exposed to 0 or 5 mM K^+ MEM under various conditions. For labeling of the cell

surface HERG channels and following the fate of labeled HERG channels, the live HERG-HEK cells were treated with an anti-HERG antibody (anti-Kv11.1; Sigma-Aldrich) for 30 minutes at room temperature. This antibody targets the external S1–S2 region of the channel. The unbound antibody was then washed with MEM, and cells were cultured in 0 or 5 mM K^+ MEM for various conditions. Antibody-labeled HERG channels were stained with Alexa Fluor 488–conjugated secondary antibody, and HERG localization was examined using a confocal microscope. Cells were shown by taking differential interference contrast (DIC) images. For membrane staining, the cells were incubated with Alexa Fluor 594–conjugated wheat germ agglutinin (WGA, 2.5 μg/ml; Invitrogen) for 1 minute at room temperature prior to cell fixation. Cells were washed and fixed with 4% ice-cold paraformaldehyde for 15 minutes, permeabilized with 0.2% Triton X-100, and blocked with 5% BSA in phosphate buffer solution. Clathrin, Rab5, CHMP3, and LAMP1 were stained with respective primary antibodies (Santa Cruz Biotechnology Inc.) and secondary antibodies. Nuclei were stained using Hoechst 33346 (0.2 μg/ml; Sigma-Aldrich). Images were acquired using a Leica TCS SP2 Multi Photon confocal microscope at Queen's University Cancer Research Institute Image Centre.

cDNAs. HERG cDNA was provided by G. Robertson (University of Wisconsin, Madison, Wisconsin, USA); KvLQT1 and KCNE1 cDNAs were provided by M. Sanguinetti (University of Utah, Salt Lake City, Utah, USA); Kv1.5 cDNA was provided by M. Tamkun (Colorado State University, Fort Collins, Colorado, USA); EAG cDNA was provided by L. Pardo (Max-Planck Institute of Experimental Medicine, Göttingen, Germany); KCNE2 cDNA was provided by S. Goldstein (University of Chicago, Chicago, Illinois, USA); and GFP-Ub cDNA was provided by N.P. Dantuma (Karolinska Institute, Stockholm, Sweden). cDNA of HERG, KvLQT1 plus KCNE1, EAG, or Kv1.5 was transfected to HEK 293 cells using Lipofectamine 2000 (Invitrogen) to express respective channels. cDNA of KCNE1, KCNE2, or GFP-Ub was transfected to HERG-HEK cells using Lipofectamine 2000 to evaluate their roles in HERG internalization under low $[K^+]_o$.

Statistics. Data represent mean ± SEM. To test for statistical significance between the control and test groups, 1-way ANOVA or 2-tailed Student's *t* test was used. A *P* value of 0.05 or less was considered significant.

Acknowledgments

We thank Wentao Li (Queen's University) for participating in some of the experiments; Pauline Smith (Queen's University) for helping with measurement of intracellular Ca^{2+} concentrations; and Keith Brunt (Queen's University) for helping with flow cytometry. We thank Larry Hryshko and Jiuyong Xie (University of Manitoba), Gui-Rong Li (University of Hong Kong, Hong Kong, Republic of China), and John Fisher (Queen's University) for reading the manuscript and providing helpful discussion. This work was supported by grants from the Canadian Institutes of Health Research (MOP 72911) and the Heart and Stroke Foundation of Ontario to S. Zhang. Z. Jia is a Canada Research Chair in Structural Biology. J. Wigle is a Manitoba Research Chair in Health Research. S. Zhang is a recipient of the Canadian Institutes of Health Research New Investigator Award.

Received for publication February 24, 2009, and accepted in revised form June 10, 2009.

Address correspondence to: Shetuan Zhang, Department of Physiology, Queen's University, 18 Stuart Street, Botterell Hall, Room 429, Kingston, Ontario K7L 3N6, Canada. Phone: (613) 533-3348; Fax: (613) 533-6880; E-mail: shetuan.zhang@queensu.ca.

1. Sanguinetti, M.C., Jiang, C., Curran, M.E., and Keating, M.T. 1995. A mechanistic link between an inherited and an acquired cardiac arrhythmia: *HERG* encodes the I_{Kr} potassium channel. *Cell.* **81**:299–307.
2. Trudeau, M.C., Warmke, J.W., Ganetzky, B., and Robertson, G.A. 1995. HERG, a human inward rectifier in the voltage-gated potassium channel family. *Science.* **269**:92–95.
3. Keating, M.T., and Sanguinetti, M.C. 2001. Molecular and cellular mechanisms of cardiac arrhythmias. *Cell.* **104**:569–580.
4. Sanguinetti, M.C., and Tristani-Firouzi, M. 2006. hERG potassium channels and cardiac arrhythmia. *Nature.* **440**:463–469.
5. Anderson, C.L., et al. 2006. Most LQT2 mutations reduce Kv11.1 (hERG) current by a class 2 (trafficking-deficient) mechanism. *Circulation.* **113**:365–373.
6. Roden, D.M., Woosley, R.L., and Primm, R.K. 1986. Incidence and clinical features of the quinidine-associated long QT syndrome: implications for patient care. *Am. Heart J.* **111**:1088–1093.
7. Compton, S.J., et al. 1996. Genetically defined therapy of inherited long-QT syndrome. Correction of abnormal repolarization by potassium. *Circulation.* **94**:1018–1022.
8. Choy, A.M., et al. 1997. Normalization of acquired QT prolongation in humans by intravenous potassium. *Circulation.* **96**:2149–2154.
9. Roden, D.M., and Hoffman, B.F. 1985. Action potential prolongation and induction of abnormal automaticity by low quinidine concentrations in canine Purkinje fibers. Relationship to potassium and cycle length. *Circ. Res.* **56**:857–867.
10. McDonald, T.V., et al. 1997. A minK-HERG complex regulates the cardiac potassium current I_{Kr}. *Nature.* **388**:289–292.
11. Abbott, G.W., et al. 1999. MiRP1 forms I_{Kr} potassium channels with HERG and is associated with cardiac arrhythmia. *Cell.* **97**:175–187.
12. Rajamani, S., et al. 2006. Specific serine proteases selectively damage KCNH2 (hERG1) potassium channels and I_{Kr}. *Am. J. Physiol. Heart Circ. Physiol.* **290**:H1278–H1288.
13. Guo, J., et al. 2007. Identification of I_{Kr} and its trafficking disruption induced by probucol in cultured neonatal rat cardiomyocytes. *J. Pharmacol. Exp. Ther.* **321**:911–920.
14. Carmeliet, E. 1998. Effects of cetirizine on the delayed K^+ currents in cardiac cells: comparison with terfenadine. *Br. J. Pharmacol.* **124**:663–668.
15. Zhang, S. 2006. Isolation and characterization of I_{Kr} in cardiac myocytes by Cs^+ permeation. *Am. J. Physiol. Heart Circ. Physiol.* **290**:H1038–H1049.
16. Zhou, Z., et al. 1998. Properties of HERG channels stably expressed in HEK 293 cells studied at physiological temperature. *Biophys. J.* **74**:230–241.
17. Gong, Q., Keeney, D.R., Molinari, M., and Zhou, Z. 2005. Degradation of trafficking-defective long QT syndrome type II mutant channels by the ubiquitin-proteasome pathway. *J. Biol. Chem.* **280**:19419–19425.
18. Laing, J.G., Tadros, P.N., Westphale, E.M., and Beyer, E.C. 1997. Degradation of connexin43 gap junctions involves both the proteasome and the lysosome. *Exp. Cell Res.* **236**:482–492.
19. van Kerkhof, P., Govers, R., Alves dos Santos, C.M., and Strous, G.J. 2000. Endocytosis and degradation of the growth hormone receptor are proteasome-dependent. *J. Biol. Chem.* **275**:1575–1580.
20. Patrick, G.N., Bingol, B., Weld, H.A., and Schuman, E.M. 2003. Ubiquitin-mediated proteasome activity is required for agonist-induced endocytosis of GluRs. *Curr. Biol.* **13**:2073–2081.
21. Gentzsch, M., et al. 2004. Endocytic trafficking routes of wild type and DeltaF508 cystic fibrosis transmembrane conductance regulator. *Mol. Biol. Cell.* **15**:2684–2696.
22. Geetha, T., and Wooten, M.W. 2008. TrkA receptor endolysosomal degradation is both ubiquitin and proteasome dependent. *Traffic.* **9**:1146–1156.
23. Zhou, Z., Gong, Q., Epstein, M.L., and January, C.T. 1998. HERG channel dysfunction in human long QT syndrome. Intracellular transport and functional defects. *J. Biol. Chem.* **273**:21061–21066.
24. Clague, M.J., and Urbe, S. 2006. Endocytosis: the DUB version. *Trends Cell Biol.* **16**:551–559.
25. Muziol, T., et al. 2006. Structural basis for budding by the ESCRT-III factor CHMP3. *Dev. Cell.* **10**:821–830.
26. Hurley, J.H. 2008. ESCRT complexes and the biogenesis of multivesicular bodies. *Curr. Opin. Cell Biol.* **20**:4–11.
27. Bonifacino, J.S., and Traub, L.M. 2003. Signals for sorting of transmembrane proteins to endosomes and lysosomes. *Annu. Rev. Biochem.* **72**:395–447.
28. Yang, T., Snyders, D.J., and Roden, D.M. 1997. Rapid inactivation determines the rectification and $[K^+]_o$ dependence of the rapid component of the delayed rectifier K^+ current in cardiac cells. *Circ. Res.* **80**:782–789.
29. Mullins, F.M., Stepanovic, S.Z., Desai, R.R., George, A.L., Jr., and Balser, J.R. 2002. Extracellular sodium interacts with the HERG channel at an outer pore site. *J. Gen. Physiol.* **120**:517–537.
30. Garcia, E., Nakhleh, N., Simmons, D., and Ramsay, C. 2008. Profound hypokalemia: unusual presentation and management in a 12-year-old boy. *Pediatr. Emerg. Care.* **24**:157–160.
31. Berthet, M., et al. 1999. C-terminal HERG mutations: the role of hypokalemia and a KCNQ1-associated mutation in cardiac event occurrence. *Circulation.* **99**:1464–1470.
32. Darbar, D., et al. 2008. Persistent atrial fibrillation is associated with reduced risk of torsades de pointes in patients with drug-induced long QT syndrome. *J. Am. Coll. Cardiol.* **51**:836–842.

33. Ficker, E., et al. 2004. Mechanisms of arsenic-induced prolongation of cardiac repolarization. *Mol. Pharmacol.* **66**:33–44.
34. Wang, L., Wible, B.A., Wan, X., and Ficker, E. 2007. Cardiac glycosides as novel inhibitors of human ether-a-go-go-related gene channel trafficking. *J. Pharmacol. Exp. Ther.* **320**:525–534.
35. Wang, L., et al. 2009. Intracellular potassium stabilizes human ether-a-go-go-related gene channels for export from endoplasmic reticulum. *Mol. Pharmacol.* **75**:927–937.
36. Ficker, E., Dennis, A.T., Wang, L., and Brown, A.M. 2003. Role of the cytosolic chaperones Hsp70 and Hsp90 in maturation of the cardiac potassium channel HERG. *Circ. Res.* **92**:e87–e100.
37. De Domenico, I., et al. 2007. The molecular mechanism of hepcidin-mediated ferroportin down-regulation. *Mol. Biol. Cell.* **18**:2569–2578.
38. Piper, R.C., and Katzmann, D.J. 2007. Biogenesis and function of multivesicular bodies. *Annu. Rev. Cell Dev. Biol.* **23**:519–547.
39. Nickerson, D.P., Russell, M.R., and Odorizzi, G. 2007. A concentric circle model of multivesicular body cargo sorting. *EMBO Rep.* **8**:644–650.
40. Kass, R.S. 2005. The channelopathies: novel insights into molecular and genetic mechanisms of human disease. *J. Clin. Invest.* **115**:1986–1989.